Laser-rf double-resonance studies of the hyperfine structure of ^{51}V

W. J. Childs, O. Poulsen,* L. S. Goodman, and H. Crosswhite
Argonne National Laboratory, Argonne, Illinois 60439
(Received 4 August 1978)

The laser-rf double-resonance technique has been used to study the hyperfine structure (hfs) of the excited $3d\,^4 4s\,^4D$ levels of ^{51}V in a continuation of earlier atomic-beam magnetic-resonance studies of the lower levels The new results make it possible for the first time to distinguish clearly between the contact hfs due to the $4s$ electron and that due to core polarization associated with the $3d$ electrons. The values found for the radial hfs integrals from a systematic analysis of both the new and earlier results are compared with the relativistic Hartree-Fock values of Lindgren and Rosén. The magnetic octopole hfs interaction is measured for one level. Hyperfine constants and lifetime information, deduced from laser-fluorescence studies, are presented for the levels $3d\,^4 4p\,^4P^o_{5/2,3/2,1/2}$ at ~ 25000 cm^{-1} excitation.

I. INTRODUCTION

For most atoms, one of the more serious problems to be overcome when subjecting high-precision optical or radio-frequency atomic spectral data to detailed theoretical analysis is the development of accurate eigenvectors for the states of interest. For the low-lying, even-parity levels of vanadium I, however, the difficulty is not too severe because of the very small departure of the levels from the LS limit, and because only a small number of configurations are important for the lower levels.[1] Because the optical emission spectrum is well understood,[2,3] such theoretical procedures as the development of eigenvectors and the evaluation of first- and second-order hyperfine effects can be carried out with enough confidence that comparison with *ab initio* calculations is meaningful. Vanadium is also an attractive atom from the experimental point of view, since many levels lie low enough to be populated easily.[1]

These features were exploited by Childs and Goodman[4,5] in 1967 in their atomic-beam magnetic-resonance measurement of the hfs of nine levels in the two multiplets $3d^3 4s^2\,^4F$ and $3d^4 4s\,^6D$. The measurements yielded the first dependable value for the nuclear electric-quadrupole moment of ^{51}V, and showed a high degree of agreement with the hfs theory. One problem this work was not able to resolve, however, was differentiation between the contact hfs of the $4s$ electron and core polarization due to the $3d$ electrons in the $3d^4 4s\,^6D$ term. The two effects could not be separated (by studies limited to the ^6D term) because of the very small departure of the levels from the LS limit, where the hfs theory predicts[5] the same J dependence for the two effects.

In this work we have extended the research to the term $3d^4 4s\,^4D$. Good agreement with the theory is achieved using new, multiconfiguration, intermediate-coupling eigenvectors, and the two sources of contact hfs are accurately resolved. A value for the magnetic-octopole hfs interaction is reported for ^{51}V. This was made possible by employing the laser-rf double-resonance technique to an atomic ^{51}V beam that contained many atoms in metastable states. The technique is characterized[6-8] by high sensitivity and high precision. In addition to the double-resonance studies, hfs and lifetime studies in the excited $3d^4 4p\,^4P^o$ manifold were carried out by Doppler-free laser fluorescence.

II. EXPERIMENTAL TECHNIQUE

A. Method

The laser-rf double-resonance technique was used to study hfs in metastable ^{51}V atoms in a vanadium beam. This technique is analogous to the traditional atomic-beam magnetic-resonance method, except that the inhomogeneous A and B magnetic deflecting fields are replaced by two laser–atomic-beam interaction regions. The laser is tuned to a particular hfs transition from a lower level $\alpha SLJIF$ to an excited level (of opposite parity) $\alpha' S' L' J' I F'$. In the first laser–atomic-beam interaction region (the pump region), the laser field is chosen sufficiently strong to empty the initial level $\alpha SLJIF$ by optical pumping. Further along the atomic beam, a second laser beam, of identical frequency but much weaker than the pump beam, is used to probe atoms of the beam. No fluorescence is observed from this second interaction (probe) region since no atoms of the beam remain in the lower hfs level to absorb the probe beam.

Fluorescence will be observed from the probe region only if rf transitions between the two interaction regions repopulate the lower hfs level. The arrangement is ideally suited to detect rf transi-

tions between different hyperfine (F) levels within the lower state, that is, transitions of the type $\alpha SLJIF \pm 1 \rightarrow \alpha SLJIF$. The advantages of the laser-rf double-resonance technique are (i) it is insensitive to small drifts of the laser frequency around the optical resonance value; (ii) it can show a very high signal-to-noise ratio; (iii) Doppler shifts are negligible since they are reduced by the ratio of the rf to the optical frequency; (iv) the rf transitions take place (with the present arrangement) at zero magnetic field, thereby eliminating all uncertainties arising from the Zeeman effect. In addition, since the rf transitions occur between the two laser interaction regions, ac Stark shifts due to the laser fields play no role; these shifts can be a serious limitation in ultrahigh-resolution laser spectroscopy.

B. Apparatus

The vanadium atomic beam was produced by heating a tantalum oven by electron bombardment. The V metal was placed in a ZrO crucible inside the Ta oven. The ^4D levels studied had almost no thermal population, but a sufficient metastable population was achieved by allowing the electrons heating the oven to intersect the atomic beam immediately in front of the oven orifice.

The laser used was a coherent radiation model 599 dye laser actively stabilized on a temperature-regulated reference cavity. The laser beam was split into two beams (pump and probe) which intersected the atomic beam orthogonally. The two interaction regions were about 20 cm apart. The laser power was typically 6 W/cm^2 in the first interaction region (pump region), and 6×10^{-2} W/cm^2 in the second region (probe region). The fluorescence emitted in the probe region was detected by a Peltier-cooled, photon-counting photomultiplier tube, and the counts were stored in a multichannel scaler.

C. Procedure

The experimental procedure consisted of two steps. The first step was to find and identify the particular transition $\alpha SLJ \rightarrow \alpha' S'L'J'$ sought. The wavelength of the laser was set to within 1 Å with a 0.5-m monochromator. A series of quick 30-GHz single-frequency scans around this wavelength then revealed the transition by producing fluorescence when on resonance. In the first step, the laser beam through the pump region was blocked. The fluorescence emitted as a function of laser wavelength was recorded on a strip chart. The spectra obtained were then identified and analyzed to yield the magnetic-dipole hfs constant A and the electric-quadrupole hfs constant B for both the lower (initial) and upper (final) states. The incremental frequency scale for these laser scans was provided by analyzing the laser light using a 25-cm, thermally isolated, confocal Fabry-Perot, so that markers were obtained every free spectral range (FSR) (300 MHz). The FSR had earlier been calibrated[8] with precisely known hfs intervals in ^{147,149}Sm.

The lines actually used to determine the hfs were 6002.6 Å ($^4D_{3/2} \rightarrow {}^4P_{5/2}$, 6081.4 Å ($^4D_{3/2} \rightarrow {}^4P_{3/2}$), 6090.2 Å ($^4D_{7/2} \rightarrow {}^4P_{5/2}$), 6111.6 Å ($^4D_{1/2} \rightarrow {}^4P_{1/2}$), 6119.5 Å ($^4D_{5/2} \rightarrow {}^4P_{3/2}$), and 6135.4 Å ($^4D_{3/2} \rightarrow {}^4P_{1/2}$).

The second step consisted of setting the laser frequency to a particular hfs component $\alpha SLJIF \rightarrow \alpha' S'L'J'IF'$ within the line, unblocking the pump beam, and observing the fluorescence intensity (over a broad wavelength region that included the laser wavelength) as a function of the applied rf frequency. The rf frequency range that had to be scanned was typically limited to ±2 MHz because of the high quality of the optical values of A, B determined above from step 1. The FWHM typically observed for the rf transitions was 20 kHz, and the precise hfs intervals thereby established for the lower state provided an accurate frequency calibration for the laser frequency scans of step 1. In this way, it was possible to refine substantially the precision attainable for the hfs constants of the upper state in each transition.

III. EXPERIMENTAL RESULTS

In this work, the zero-field hyperfine intervals of the $3d^44s\ ^4D_{7/2,5/2,3/2}$ levels were measured with the laser-rf double-resonance technique. The same method was used to remeasure one $\Delta F = \pm 1$ hfs interval in the previously measured (Ref. 4) $3d^34s^2\ ^4F$ multiplet, and excellent agreement with the earlier results was found.

The single $F = 4 \leftrightarrow 3$ hfs interval in the $3d^44s\ ^4D_{1/2}$ state could not be measured with the double-resonance method because the rf transition probability is proportional to the square of the Landé g_J value for the state, and it happens to be almost exactly zero. For this reason, this one interval was measured only by the laser-fluorescence method, to a precision of 0.3%. In addition, all the hfs intervals in the $3d^44P^o_{1/2,3/2,5/2}$ levels were measured by analysis of the optical fluorescence spectra.

A. $\Delta F = \pm 1$ intervals in the $3d^44s\ ^4D$ levels

Figure 1 shows the optical spectrum of the $3d^44s\ ^4D_{3/2} \rightarrow 3d^44p\ ^4P^o_{1/2}$ transition [Fig. 1(a)] and the rf spectra of the three hfs intervals in the $^4D_{3/2}$ level [Figs. 1(b), 1(c), and 1(d)]. Because of the short lifetime of the upper state and the very small hfs separations of the lower level, the hfs

components are only partially resolved in Fig. 1(a). Nevertheless this was not a problem, and the double-resonance technique established the hfs separations very cleanly to a precision of better than 1 kHz. Table I shows the observed hfs intervals, together with the corresponding results for the other states of the ^4D term. The "uncorrected" values of the hfs constants A and B are obtained from these observed hfs intervals by comparing them with the intervals predicted by the standard hyperfine-structure Hamiltonian[9]

$$\mathcal{H}_{\rm hfs} = AI\cdot J + BQ_{\rm op} + C\Omega_{\rm op};$$

the procedures are discussed in detail in Ref. 9.

B. hfs of the $3d^4 4p\ ^4P^o$ levels

Table II gives the A and B values found for the $3d^4 4p\ ^4P^o_{1/2,3/2,5/2}$ levels, determined from the optical fluorescence spectra. Figure 1(a) shows one such spectrum as an example.

The linewidth evident in Fig. 1(a) gives information on the natural lifetime of the upper level. After taking account of the laser linewidth (~2 MHz), the Doppler width (~4 MHz), and the laser power used, the lifetime of the $3d^4 4p\ ^4P^o_{3/2}$ level is deduced to be 9.5 ± 2.0 ns.

IV. THEORY AND INTERPRETATION

A. Introduction

The principal purpose of the theoretical analysis is to extract from the relatively large number of measured hfs constants (including those measured earlier), a smaller number of more general radial parameters that can be compared with *ab initio* calculations. Knowledge of these quantities then makes it possible to predict hfs and other properties of many levels of the atom.

The first step in such an anlaysis is the development of a set of multiconfiguration, intermediate-coupling eigenvectors for the states of interest. With these eigenvectors, parametrized theoretical expressions for the measured hfs constants are developed for comparison with the observed values. For each state of interest, corrections for the effects of hfs interactions with neighboring levels[9] must be evaluated (off-diagonal or second-order hfs) before making the comparison with theory. The parameters in the hfs theory are then evaluated by least-squares fitting the theoretical expressions for the hfs constants to the corrected measured values.

B. Eigenvectors

To develop the eigenvectors needed, the matrix of all levels of the three lowest, even-parity configurations of V I($3d^3 4s^2$, $3d^4 4s$, and $3d^5$) was

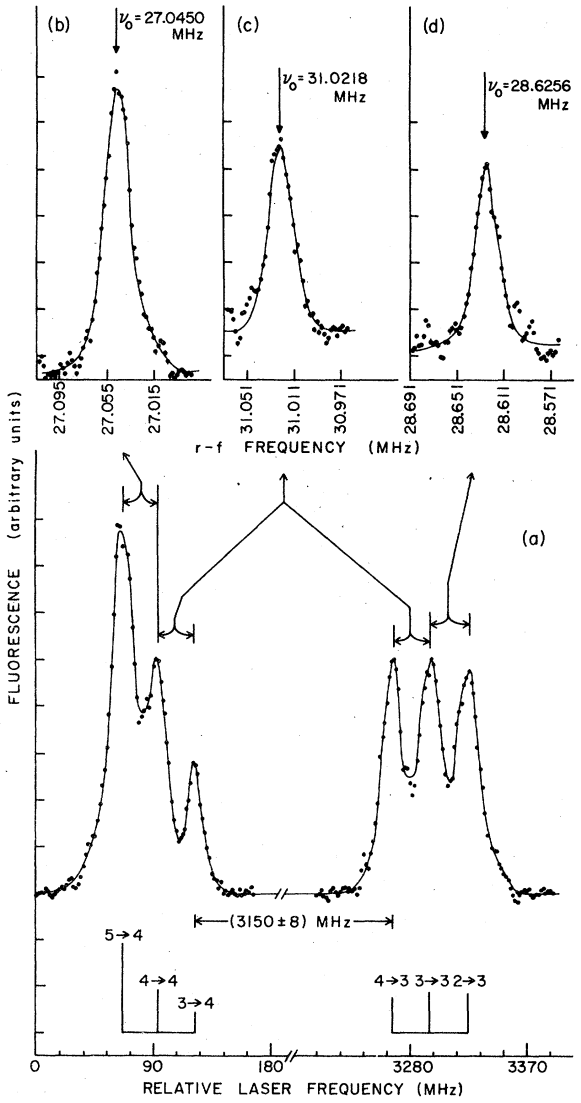

FIG. 1. Experimental results for the transition $3d^4 4s\ ^4D_{3/2} \rightarrow 3d^4 4p\ ^4P^o_{1/2}$. (a) Shows the optical-fluorescence spectrum; the theoretical intensities and identification of the components are shown below. The resolution in this spectrum is limited by the 9.5-ns natural lifetime of the $^4P^o_{1/2}$ level, as determined in this work. The broadening due to laser power was carefully studied. The laser power in this case was ~10 mw/cm^2. In (b), (c), and (d) are shown the rf resonances, all obtained in a few minutes of signal averaging, despite the fact that the hfs components are not fully resolved in the optical spectrum.

diagonalized. In addition to the usual Coulomb and spin-orbit parameters, the matrix elements contained other parameters to allow for the effects of configuration interaction with distant configurations not explicitly included in the basis set. Of the total of 28 parameters, 14 were varied itera-

TABLE I. Observed rf frequencies (hyperfine intervals) in the $3d^4 4s\,{}^4D_J$ fine-structure multiplet. The A and B values are obtained through least-squares fits to the observed rf frequencies, using the usual hfs Hamiltonian. The $3d^4 4s\,{}^4D_{1/2}$ splitting is obtained from optical-fluorescence data, since a zero magnetic moment prohibits magnetic rf transitions.

Level	Excitation energy (cm^{-1})	$F \leftrightarrow F$	Observed rf frequency (MHz)	Uncorr. A (MHz)	Uncorr. B (MHz)
$^4D_{7/2}$	8715.76	0 ⟷ 1	161.270(2)	−160.2192	10.2287
		1 ⟷ 2	322.3172(5)		
		2 ⟷ 3	482.9548(5)		
		3 ⟷ 4	642.9634(5)		
		4 ⟷ 5	802.1384(5)		
		5 ⟷ 6	960.2732(5)		
$^4D_{5/2}$	8578.53	1 ⟷ 2	286.5262(5)	−143.4320	−1.1959
		2 ⟷ 3	429.9116(5)		
		3 ⟷ 4	573.4463(5)		
		4 ⟷ 5	717.1924(5)		
		5 ⟷ 6	861.2195(5)		
$^4D_{3/2}$	8476.23	3 ⟷ 2	28.6256(5)	6.9658	−10.8535
		4 ⟷ 3	31.0218(5)		
		5 ⟷ 4	27.0450(5)		
$^4D_{1/2}$	8413.00	3 ⟷ 4	5106(16)	1276(5)	

tively to obtain a least-squares fit to the energies of the 56 levels whose identities were considered established. The final fit to all the fine-structure energies is within an rms error of 116 cm^{-1}, and the fit to the levels studied in this work is very much better still. The basis set would have to be expanded to include still higher-lying configurations explicitly to obtain a significantly better fit. Comparison of the g_J values predicted by the resulting eigenvectors with the measured values shows good agreement up to around 15 000 cm^{-1}, well above the region examined in this study. Such good agreement, however, can be expected for the low levels of vanadium, for which the departure from the LS limit is very small.

The eigenvector obtained for the $3d^4 4s\,{}^4D_{3/2}$ state.

$$
\begin{aligned}
|{}^4D_{3/2}\rangle = {} & 0.995894\,|d^4({}^5D), s; {}^4D\rangle \\
& -0.082507\,|d^5\,{}^4D\rangle \\
& -0.016231\,|d^4({}^3P1), s; {}^2P\rangle \\
& -0.015501\,|d^3 s^2\,{}^4P\rangle \\
& +0.015439\,|d^4({}^3D), s; {}^4D\rangle \\
& +0.013262\,|d^4({}^3P2), s; {}^2P\rangle + \cdots \qquad (1)
\end{aligned}
$$

is typical, although the $d^4 s\,{}^6D_J$ and $d^3 s^2\,{}^4F_J$ states lie closer still to the LS limit. (The numbers immediately to the right of the ^3P term labels in Eq. (1) employ the convention of Nielson and Koster[10] to remove any ambiguity in the identification of the basis states.)

Owing to the limited amount of data available, no effort was made to develop eigenvectors for the excited, odd-parity $3d^4 4p\,{}^4P_J$ levels reached by laser excitation. Because of the many interacting levels in this region[1] (~25 000 cm^{-1}), good eigenvectors would be an essential prerequisite for interpretation of the hfs.

C. Theoretical expressions for the hfs constants

Sandars and Beck[11] have published the effective operators required for the relativistic hyperfine interaction in many-electron atoms. For each order of the hyperfine interaction (dipole, quadrupole, or octopole, for example), three radial integrals are required for each partially filled electron shell; we shall regard these integrals as parameters. In addition, the value of any given parameter may in principle depend on which configuration one is considering. Expressions for the matrix elements of these hfs operators have been given[9,12] for configurations of the classes l^N and

TABLE II. A and B values for the $3d^4 4p\,{}^4P^o_J$ multiplet, obtained from least-squares fits to the hfs intervals measured in the optical fluorescence spectra.

Level	Energy (cm^{-1})	A (MHz)	B (MHz)
$z\,{}^4P^o_{5/2}$	25131.01	−89.8(6)	8(5)
$z\,{}^4P^o_{3/2}$	24915.14	−286.4(6)	−6(5)
$z\,{}^4P^o_{1/2}$	24770.68	−795.2(20)	

$l^N l'$, in which d^3s^2, d^4s, and d^5 are included. Thus, for the complete eigenvector for the $^4D_{3/2}$ level, for example, one obtains a theoretical expression for the magnetic-dipole A factor that is linear in 12 radial parameters, and one for the electric-quadrupole B factor that is linear in 11. Since the cross-configuration hfs contributions are proportional to the almost vanishing radial integral $\langle 3d|r^{-3}|4s\rangle$, these terms may be dropped. In addition, we have made the simplifying assumption that the value of a given parameter is independent of the configuration in which it occurs. With these simplifications, one obtains, for example, in intermediate coupling the expression

$$A(^4D_{3/2}) = 0.799716\, a^{01}_{3d} - 0.240975\, a^{12}_{3d} + 0.242392\, a^{10}_{3d} - 0.042108\, a^{10}_{4s}, \quad (2)$$

in which the parameters a^{k_s,k_l}_{nl} are defined in Ref. 9. This may be compared with the almost identical expression derived for the LS limit

$$A^{LS}(^4D_{3/2}) = 0.8\, a^{01}_{3d} - 0.24\, a^{12}_{3d} + 0.24\, a^{10}_{3d} - 0.04\, a^{10}_{4s}. \quad (3)$$

It may be shown that in the LS limit, the contact hfs parameters a^{10}_{3d} and a^{10}_{4s} are linearly dependent, and may be replaced, for the d^4s ^4D multiplet, by the single parameter $a^{10}_{4s} - 6a^{10}_{3d}$, and for the d^4s ^6D term by $a^{10}_{4s} + 4a^{10}_{3d}$. Because these multiplets are in fact so close to the LS limit, it is difficult to separate the effects of the two contact parameters when either multiplet is considered separately.

Having obtained expressions of the type (2) for the A and B factors of the V I levels of interest, one can vary the radial parameters in them to make a least-squares fit to the measured values. When this is done for the d^3s^2 ^4F multiplet, one finds parameter values very close to those published earlier.[5] When one makes such fits for the d^4s ^6D or ^4D terms separately, one finds that the interdependence of the a^{10}_{3d} and a^{10}_{4s} parameters makes it impossible to obtain physically sensible values. Nevertheless the quantity $a^{10}_{4s} + 4a^{10}_{3d}$ computed from the values found for a^{10}_{3d} and a^{10}_{4s} in fitting the ^6D A values is in close agreement with the published value[5] for the contact parameter.

When the hfs constants of the two multiplets d^4s ^6D and ^4D are fitted simultaneously, however, reliable values for the two contact parameters are found. The preliminary values found in this way for the dipole hfs parameters a^{01}_{3d}, a^{12}_{3d}, a^{10}_{3d} and a^{10}_{4s} are 307, 270, −189, and 3053 MHz, respectively, for the $3d^4 4s$ configuration. For the $3d^3 4s^2$ configuration, a^{01}_{3d}, a^{12}_{3d}, and a^{10}_{3d} have the values 353, 317, and −64 MHz, respectively; the parameter a^{10}_{4s} is not needed for this configuration.

D. Second-order hfs corrections

Before the values obtained for the hfs constants can be used to reveal the underlying hfs radial parameters, they must be corrected for the effects of hfs interactions with nearby states. These hfs perturbations[13] are evaluated for each hfs level $\alpha SLJIF$ by second-order perturbation theory according to the relation

$$\delta E(\alpha \mathcal{S}\mathcal{L}JIF) = \sum{}' \frac{|\langle \alpha \mathcal{S}\mathcal{L}JIFM|\mathcal{H}_{\rm hfs}|\alpha'\mathcal{S}'\mathcal{L}'J'IFM\rangle|^2}{E(\alpha \mathcal{S}\mathcal{L}J) - E(\alpha'\mathcal{S}'\mathcal{L}'J')}.$$

The prime indicates that all states different from the one for which the corrections are being calculated are included in the sum, and the script $\mathcal{S}$ and $\mathcal{L}$ indicate that the corrections may have to be evaluated in intermediate coupling.

Because of the very small size of the electric-quadrupole moment of ^{51}V, only the dipole operator need be considered in making the corrections. Perturbations involving hfs interactions between different configurations may also be disregarded because of the extremely small magnitude of the integral $\langle 3d|r^{-3}|4s\rangle$ to which the matrix elements are proportional. Corrections for the $3d^3 4s^2$ ^4F states were made in the LS limit since these states are more than 99.9% pure. In addition, calculations showed that terms of $3d^3 4s^2$ other than the ground ^4F multiplet made negligible contributions. The corrections calculated for the ^4F term are thus nearly identical to those reported[5] earlier.

Both the ^6D and ^4D multiplets of $3d^4 4s$ must be considered when making second-order hfs corrections to any level of either term. Since the second second-order effects of the higher-lying ^4D term on the hfs of the ^6D levels were ignored in the previous analysis,[5] the present values for the corrected ^6D hfs constants differ slightly from those reported earlier. The contributions of still higher terms of $3d^4 4s$ on the corrections for the ^4D and ^6D levels were also included in the present analysis, and for the ^4D levels (whose eigenvectors differ much more from the LS limit than do those for ^6D), the corrections were made in intermediate coupling.

The radial parameter values used in making the corrections were obtained as discussed above. Refitting the theoretical expressions for the hfs constants to the *corrected* experimental A and B values then gives refined values for the parameters, and this procedure is iterated until no further significant change occurs. The final values obtained for the hfs parameters will be given below.

The second-order corrections to the hfs of the $3d^4 4s$ $^4D_{3/2}$ state are so large as to be of special interest. The three observed hfs intervals, taken

from Table I, along with the second-order corrections and the final, corrected intervals that would be observed if all other levels were infinitely far removed are shown in Table III. Although the corrected intervals are almost exactly in the ratio 5:4:3 as required by the dipole interval rule (the quadrupole interaction is of minor importance in ^{51}V), the three observed intervals are nearly equal. The unusually large perturbations are due to the very small spacings within the $3d^4 4s\ ^4D$ multiplet.

E. Electric-quadrupole hfs of $3d^4 4s\ ^4D_{3/2}$

It follows from the multiconfiguration, intermediate-coupling eigenvector of Eq. (1) for the $^4D_{3/2}$ state that the B factor can be expressed as

$$B(^4D_{3/2}) = 0.000\,103 b_{3d}^{02} + 0.029\,964 b_{3d}^{13} + 0.046\,695 b_{3d}^{11} \quad (4)$$

in which a given parameter is assumed to have the same value in the configurations $3d^3 4s^2$, $3d^4 4s$, and $3d^5$. [The quadrupole parameters in Eq. (4) are defined in Ref. 9]. The reason the nonrelativistic and normally dominant term b_{3d}^{02} has such a small coefficient is that in the LS limit it is proportional to

$$\begin{Bmatrix} J & J & 2 \\ L & L & S \end{Bmatrix} = \begin{Bmatrix} \frac{3}{2} & \frac{3}{2} & 2 \\ 2 & 2 & \frac{3}{2} \end{Bmatrix} = 0$$

for the $^4D_{3/2}$ state, and the eigenvector contains almost no admixture.

The parameter b_{3d}^{02} has the value −24.6 MHz, and the approximate values $b_{3d}^{13} = -0.81$ MHz and $b_{3d}^{11} = 0.35$ MHz may be taken from the relativistic Hartree-Fock calculations of Lindgren and Rosén[14] (LR) to yield the value

$$B(^4D_{3/2}) = -0.010 \pm 0.004 \text{ MHz}, \quad (5)$$

which differs from zero primarily through relativistic effects (the nonzero value of the B factor is entirely relativistic if spin-orbit mixing is regarded as a relativistic effect).

That the B value for $d^4 s\ ^4D_{3/2}$ is indeed very small is shown by the results of even the crudest application of the second-order corrections, which reduces the B factor from the uncorrected value −10.9 MHz to the (crudely corrected) value −0.2 MHz. The fact that Eq. (5) shows the B factor of the $^4D_{3/2}$ state to be much smaller still allows us to use this information to determine and set limits on the second-order corrections. Thus the radial hfs parameter used in making the second-order corrections can be determined solely from the B factor of the $^4D_{3/2}$ state, and the results compared with the parameter values obtained above by fitting the A values for all the states. Since both the diagonal (first-order) and off-diagonal (second-order) dipole hfs are dominated by the parameter a_{4s}^{10}, we may fix the other dipole parameters at their final values ($a_{3d}^{01} = 309$ MHz, $a_{3d}^{12} = 271$ MHz, and $a_{3d}^{10} = -190$ MHz), and plot the value of $B(^4D_{3/2})$ obtained by application of the second-order corrections to the experimental value against the value of a_{4s}^{10} used in evaluating the corrections. Figure 2 shows the result; one con-

TABLE III. Zero-field $\Delta F = \pm 1$ hyperfine intervals in the $3d^4 4s\ ^4D_{3/2}$ level. It is seen that the observed intervals (in column 2) must be altered by corrections ranging up to nearly 40% for the effects of second-order hfs in order to extract the underlying hfs parameters for comparison with *ab initio* theory.

$\Delta\nu$ $F \leftrightarrow F'$	Observed hfs interval (MHz)	Second-order hfs correction (MHz)	Corrected hfs interval (MHz)
5 ↔ 4	27.045	10.271	37.316
4 ↔ 3	31.022	−1.136	29.886
3 ↔ 2	28.626	−6.245	22.381

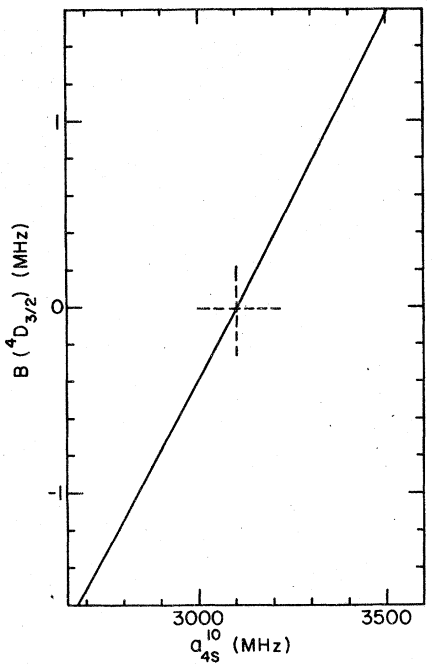

FIG. 2. Plot of the B value obtained for the $3d^4 4s\ ^4D_{3/2}$ state, as a function of the value of the principal parameter used in making the second-order hfs corrections to the observed hfs intervals. The parameter a_{4s}^{10} measures the contact dipole hfs due to the 4s-electron. The dashed lines indicate that for the value $B = -0.010$ MHz required by the theory, the parameter a_{4s}^{10} has the value 3105 MHz, in almost exact agreement with the value obtained independently from the measured A values of the ^4D levels.

TABLE IV. Final values of the hfs constants for the $3d^3 4s^2\,{}^4F$, $3d^4 4s\,{}^6D$, and $3d^4 4s\,{}^4D$ terms of ^{51}V, after correction for the effects of second-order hfs. The results for the ^4D levels are presented here for the first time; the others result from application of the present, more accurate, second-order corrections to the previously published (Ref. 4) experimental intervals.

Configuration	State	Corrected hfs constants A (MHz)	B (MHz)	C (kHz)
$3d^3 4s^2$	$^4F_{9/2}$	227.135(1)	8.243(30)	2(2)
$3d^3 4s^2$	$^4F_{7/2}$	249.752(2)	5.587(25)	−1(2)
$3d^3 4s^2$	$^4F_{5/2}$	321.251(3)	3.955(45)	0(2)
$3d^3 4s^2$	$^4F_{3/2}$	560.068(2)	3.987(25)	···
$3d^4 4s$	$^6D_{9/2}$	406.848(4)	14.041(65)	5(9)
$3d^4 4s$	$^6D_{7/2}$	382.367(2)	2.293(30)	1(3)
$3d^4 4s$	$^6D_{5/2}$	373.526(2)	−5.004(30)	0(2)
$3d^4 4s$	$^6D_{3/2}$	405.642(4)	−6.985(15)	···
$3d^4 4s$	$^6D_{1/2}$	751.529(7)	0	0
$3d^4 4s$	$^4D_{7/2}$	−160.187(2)	13.874(25)	0.26(40)
$3d^4 4s$	$^4D_{5/2}$	−143.256(2)	5.145(20)	−0.27(8)
$3d^4 4s$	$^4D_{3/2}$	7.465(5)	−0.010(6)	−1.66(14)
$3d^4 4s$	$^4D_{1/2}$	1277.2 ± 4.0	0	0

cludes that

$$a^{10}_{4s} = 3105 \pm 30 \text{ MHz},$$

based solely on the second-order hfs corrections to the B factor of the $^4D_{3/2}$ state. This may be compared with the value 3061 ± 11 MHz obtained from fitting the first-order, dipole A factors of all nine ^6D and ^4D levels. The better than 1.5% agreement is indeed remarkable.

Having determined the value of the dominant parameter in the second-order hfs corrections accurately, the corrections were then recalculated for all the states of interest in ^{51}V. Table IV gives the final corrected values for the hfs constants of the $3d^4 4s\,{}^4D$ levels reported herein, and also the results of applying the present, more accurate corrections to the earlier measurements of Childs and Goodman[4] for the $3d^4 4s\,{}^6D$ and $3d^3 4s^2\,{}^4F$ terms.

The theoretical expressions for the A and B factors were then fitted to these corrected hfs constants to determine the best-fit values of the hfs radial parameters. The quality of the fits was high, and the values obtained for the parameters are therefore believed to be trustworthy.

F. hfs radial parameter values

The final values found for the radial dipole hfs parameters are given in Table V. The small departure of $\alpha \equiv a^{01}_{3d}/a^{12}_{3d}$ from unity ($\alpha = 1.11$ for $3d^3 4s^2$ and 1.14 for $3d^4 4s$) is virtually identical to that reported earlier, and is in disagreement with the Lindgren and Rosén[14] (LR) relativistic Hartree-Fock result of 0.98, probably due to configuration interaction. For the light vanadium atom, LR shows that relativistic effects should amount to less than 5% of the observed value of a^{10}_{3d} for $3d^3 4s^2$; their calculation of the configuration interaction contribution (mostly core polarization) differs from experiment by about 33%. The relativistic Hartree-Fock value found by LR for a^{10}_{4s} in $3d^4 4s$ is 3173 MHz, which agrees with the new experimental result to within 2%. The previously reported[5] experimental value (2301 MHz for $3d^4 4s\,{}^6D$) includes core polarization due to the $3d$ electron shell.

The new experimental ratio $b^{02}_{3d}(3d^3 4s^2)/b^{02}_{3d}(3d^4 4s) = 1.18$ agrees to within 1% with the LR relativistic HF result,[14] but the experimental values for the purely relativistic quadrupole parameters b^{13}_{3d} and b^{11}_{3d} are very far from the relativistic HF values[14]

TABLE V. Final values of the radial hfs parameters found for the low levels of the $3d^3 4s^2$ and $3d^4 4s$ configurations of ^{51}V. These values are compared with the relativistic Hartree-Fock calculations of Lindgren and Rosén (Ref. 14) in the text.

Parameter	Order of hfs interaction	Parameter value (MHz) $3d^3 4s^2$	$3d^4 4s$
a^{01}_{3d}	Dipole	353(3)	309(5)
a^{12}_{3d}	Dipole	317(15)	271(20)
a^{10}_{3d}	Dipole	−64(3)	−190(5)
a^{10}_{4s}	Dipole	···	3105(30)
b^{02}_{3d}	Quadrupole	−29.0(2)	−24.6(2)
b^{13}_{3d}	Quadrupole	1.3(4)	0.6(9)
b^{11}_{3d}	Quadrupole	− 0.4(2)	0.1(7)

−0.81 and +0.35 MHz, respectively. The B values in ^{51}V are very small, however, and the relativistic parameters b_{3d}^{13} and b_{3d}^{11} are very sensitive to small changes in any part of the analysis, in contrast to the situation for the nonrelativistic parameter b_{3d}^{02}.

G. Magnetic-octopole hyperfine interaction

Because of the high precision of the present hfs measurements of the $3d^4 4s\ ^4D$ levels, there is the possibility of observing magnetic-octopole or electric-hexadecapole interactions. The principal problem is that the second-order hfs corrections to the observed hfs intervals must be made accurately and dependably. The only state for which a substantial apparent octopole interaction is found is $3d^4 4s\ ^4D_{3/2}$ (no higher-order interactions are possible for $J=\frac{3}{2}$). In assigning an uncertainty to the present value $C(^4D_{3/2}) = -1.7$ kHz (from Table IV), analysis shows that the part due to experimental uncertainty is only about ±0.1 kHz. One would expect that the principal cause of uncertainty would be in the second-order corrections to the hfs intervals of the $^4D_{3/2}$ state. However, if a plot is made of $C(^4D_{3/2})$ versus a_{4s}^{10}, similar to that for $B(^4D_{3/2})$ in Fig. 2, it is found that the uncertainty in C corresponding to a range of a_{4s}^{10} of ±310 MHz (±10%) is only ±0.11 kHz.

Since the octopole C factor of the $^4D_{5/2}$ state also appears to be nonzero (Table IV), it is of interest to calculate the expected J dependence of the C factors for comparison with the experimental values. From the effective octopole operators given by Sandars and Beck[11] and discussed at length by LR[14] and by Armstrong,[15] it follows that for the $3d^4(^5D), 4s\ ^4D$ term we have

$$\begin{aligned} C(^4D_{7/2}) &= +\tfrac{13}{35}\, c_{3d}\,, \\ C(^4D_{5/2}) &= -\tfrac{82}{245}\, c_{3d}\,, \\ C(^4D_{3/2}) &= -\tfrac{46}{245}\, c_{3d}\,, \end{aligned} \tag{6}$$

in which the nonrelativistic LS limit is used and the parameter c_{3d} is as defined by LR.[14] The fact that the experimental value of $C(^4D_{3/2})$ is larger than $C(^4D_{5/2})$ disagrees with the theory and is not understood. The insensitivity of $C(^4D_{3/2})$ to very large changes in the strength of the second-order corrections appears to rule out uncertainties of this type as the explanation of the discrepancy.

V. CONCLUSIONS

The principal conclusion from the present work is that studying higher levels of a configuration in which only lower levels have previously been examined can provide new atomic-structure information. Thus we have succeeded in distinguishing between the $3d$- and $4s$-electron contributions to the $3d^4 4s$ contact hfs, and, in addition, shown how different the $3d$ part is in the $3d^3 4s^2$ and $3d^4 4s$ configurations. These results are in qualitative agreement with the relativistic theory when configuration-interaction effects are included.

That one obtains almost identical values for the $4s$-electron contact hfs from consideration of the first-order, dipole hfs of several levels and from the second-order, quadrupole hfs of a single level is remarkable. Although the self-consistency of the results under close theoretical analysis is in general extremely good, some problems remain unaccounted for. In particular, the magnitudes of the relativistic quadrupole hfs integrals, and the J dependence of the magnetic-octopole hfs interaction constants are puzzling. It is clear that additional studies of still higher-lying levels, including levels of $3d^3 4s^2$ and hopefully $3d^5$, would be of great value.

Another conclusion one might draw is that high-precision hfs results are essential for detailed structural studies of this kind. Laser-fluorescence studies yielding results at the 0.5% level will often fail to reveal the details of greatest interest. The very high precision of the laser-rf double-resonance technique appears to be ideally suited to such studies.

ACKNOWLEDGMENTS

One of the authors (O. P.) acknowledges partial support from the Danish Natural Science Research Council. Work was performed under the auspices of Basic Energy Sciences of the Dept. of Energy.

*Permanent address: Institute of Physics, University of Aarhus DK8000 Aarhus C, Denmark.

[1] *Atomic Energy Levels*, edited by C. E. Moore, Natl. Bur. Std. Circ. No 467 (U. S. GPO, Washington, D. C., 1949), Vol. I.

[2] D. S. Davies and K. L. Andrew, J. Opt. Soc. Am. 68, 206 (1978). References to earlier work may be found here and in Ref. 3.

[3] D. S. Davies, K. L. Andrew, and J. Verges, J. Opt. Soc. Am. 68, 235 (1978).

[4] W. J. Childs and L. S. Goodman, Phys. Rev. 156, 64 (1967).

[5] W. J. Childs, Phys. Rev. 156, 71 (1967).

[6] S. D. Rosner, R. A. Holt, and T. D. Gaily, Phys. Rev. Lett. 35, 785 (1975).

[7] W. Ertmer and B. Hofer, Z. Phys. A 276, 9 (1976).

[8] W. J. Childs, O. Poulsen, and L. S. Goodman, Phys. Rev. A (to be published).

[9]W. J. Childs, Case Stud. Atom. Phys. 3, 215 (1973).
[10]C. W. Nielson and G. F. Koster, *Spectroscopic Coefficients for the p^n, d^n, and f^n configurations* (MIT, Cambridge, Mass. 1963).
[11]P. G. H. Sandars and J. Beck, Proc. R. Soc. Lond. Ser. A 289, 97 (1965).
[12]W. J. Childs, Phys. Rev. A 2, 316 (1970).
[13]See pp. 271–280 of Ref. 9.
[14]I. Lindgren and A. Rosén, Case Stud. Atom. Phys. 4, 197 (1974); see pp. 250–260.
[15]L. Armstrong, *Theory of the Hyperfine Structure of Free Atoms* (Wiley-Interscience, New York, 1971).